Eur. Phys. J. A **17**, 523–528 (2003)
DOI 10.1140/epja/i2002-10159-8

THE EUROPEAN PHYSICAL JOURNAL A

Configuration assignments of yrare high-spin structures in ^{126}Cs

X.-F. Li[1], Y.-J. Ma[1,a], Y.-Z. Liu[1,2], J.-B. Lu[1], G.-Y. Zhao[1], L.-C. Yin[1], R. Meng[1], Z.-L. Zhang[1], L.-J. Wen[1], X.-H. Zhou[2], Y.-X. Guo[2], X.-G. Lei[2], Z. Liu[2], Y. Zheng[2], and J.-J. He[2]

[1] Department of Physics, Jilin University, Changchun 130023, PRC
[2] Institute of Modern Physics, Chinese Academy of Science, Lanzhou 73000, PRC

Received: 16 September 2002 / Revised version: 10 March 2003 /
Published online: 1 July 2003 –
Communicated by D. Guerreau

Abstract. High-spin states in ^{126}Cs were populated in the reaction ^{116}Cd(^{14}N, 4n) at a beam energy of 65 MeV. About 50 new transitions were placed in a level scheme that consists of six rotational structures, three of which have been observed for the first time. The newly observed bands and a previously reported but uninterpreted band were assigned configurations based on their population, aligned angular momentum, energy signature splitting and $B(M1)/B(E2)$ ratios (for the strongly coupled bands).

PACS. 21.10.Re Collective levels – 27.60.+j $90 \leq A \leq 149$

Doubly odd Cs isotopes have been extensively studied by means of in-beam γ-ray spectroscopy. In ^{126}Cs, three rotational bands had previously been established by Komatsubara *et al.* [1] following the ^{116}Cd(^{14}N, 4n) reaction, but only the yrast band was discussed in detail in ref. [1]. Additional discussion [2] concerning the yrast band was recently made on the basis of systematic study, proposing a spin assignment that, however, differs from that deduced in ref. [1]. To improve the understanding of the previously observed bands and to search for new bands, the level structure of ^{126}Cs has been investigated by spectroscopic measurements in the present work.

Excited states in ^{126}Cs were populated through the ^{116}Cd(^{14}N, 4n) fusion-evaporation reaction at a beam energy of 65 MeV. The beam was provided by the Heavy Ion Accelerator of the Institute of Modern Physics at Lanzhou, China. The target of ^{116}Cd was a self-supporting foil of 2.5 mg/cm^2 in thickness. Gamma-ray coincidences were measured with ten Compton-suppressed HPGe detectors and one planar HPGe detector. About 120 million events requiring two or more detectors fire in coincidence within 80 ns were accumulated. In the offline analysis, spectra recorded from the ten Compton-suppressed detectors were corrected for Doppler shift depending on detector angles. They were then sorted into an E_γ-E_γ matrix for the determination of γ-γ coincidence relationships. For angular-correlation information a DCO matrix was created with the forward and backward detectors on one axis and the near-90° detectors on the other axis.

[a] Correspondence author; e-mail: yjma@public.cc.jl.cn

The present work confirms most of the previously reported [1] levels and transitions in ^{126}Cs. In addition, three new yrare rotational structures have been identified. A partial level scheme of ^{126}Cs showing the newly identified bands (labeled 3, 5 and 6) together with the previously reported bands (labeled 1, 2 and 4) is presented in fig. 1. About 50 new transitions have been added into the level scheme. Data for transitions shown in fig. 1 are summarized in table 1.

In ref. [1], band 2 was assigned to the $\pi h_{11/2} \otimes \nu h_{11/2}$ configuration, and its bandhead (assumed to be the state fed by the 141 and 478 keV transitions for convenience of discussion) was located at an excitation energy of 760 keV and the bandhead spin was tentatively assigned to be 5 $\hbar$. In a recent systematic study [2] of the $\pi h_{11/2} \otimes \nu h_{11/2}$ bands in odd-odd $^{118\text{-}132}$Cs isotopes including ^{126}Cs, a new spin assignment of $I = 9$ was proposed for the bandhead instead of the previous $I = 5$ assignment. In the present study, neither of the above spin assignments is confirmed due to poor statistics, which prevents us from obtaining reliable DCO ratios of some crucial γ-transitions de-exciting band 2 to lower states. The spin assignment shown in fig. 1 for band 2 is proposed *tentatively* based on ref. [2].

In the work by Komatsubara *et al.* [1], a decoupled band was observed to decay strongly to band 2 at low spins. In our experiment, coincidence between the 427 and 672 keV γ-rays (cf. fig. 1) was observed clearly, and a band that consists of two decay sequences at low spins, *i.e.* the band labeled 1 in fig. 1, has therefore been developed from the above-mentioned decoupled band. While the measured

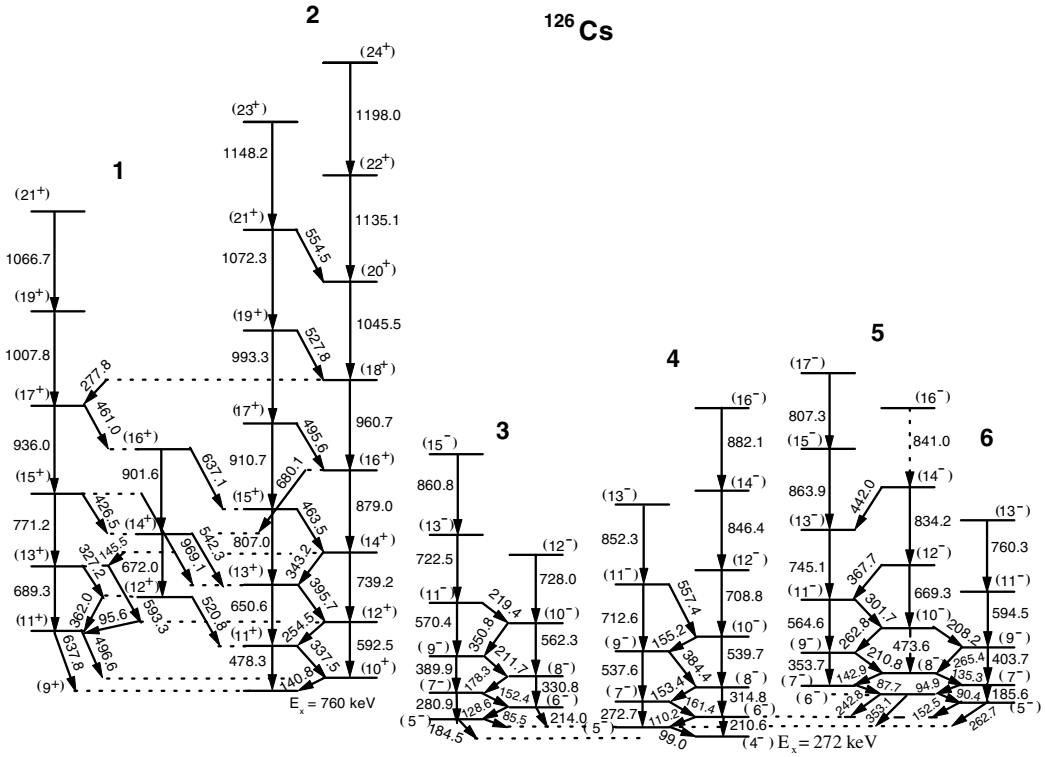

Fig. 1. Partial level scheme of ^{126}Cs showing the high-spin rotational bands. The excitation energies shown for the bandhead states of bands 2 and 4 are taken from ref. [1].

DCO ratios ($R_{\rm DCO} \approx 0.5$–0.7; see table 1) of the 497, 521 and 542 keV linking transitions from band 1 to band 2 are consistent with $\Delta I = 1$ multipolarity assignments for these transitions, the measured DCO ratio ($R_{\rm DCO} = 1.05 \pm 0.22$) of the 638 keV crossover transition (cf. fig. 1) strongly suggests that this transition is of $E2$ character. Thus, band 1 has been assigned positive parity and the relative spins as shown in fig. 1. Presumably, band 1 is a chiral partner of band 2 like the chiral bands recently proposed in the neighboring ^{128}Cs [3] and ^{130}Cs [4], as has been addressed in paper [5].

The possible spin/parity of the bandhead (assumed to be the state fed by the 99 and 210 keV transitions) of band 4 was not discussed in ref. [1], but its excitation energy was determined to be 272 keV [1]. In another work [6] by Komatsubara *et al.*, this $E_x = 272$ keV state was identified to be an isomer with $T_{1/2} \geqslant 1\,\mu$s. In the present study, by setting gates on the transitions near the bottom of band 4, three new rotational structures, *i.e.* the bands labeled 3, 5 and 6 in fig. 1, have been established. In view of the transitions connecting these new bands to band 4 and the multipolarity of the 184.5, 214.0, 353.1 and 262.7 keV transitions to be dipole as inferred from the measured DCO ratios (cf. table 1), tentative relative spin assignments for bands 3, 4, 5 and 6 have been assigned, as displayed in fig. 1.

Near the Fermi surface of ^{126}Cs, the shell model orbitals available are $h_{11/2}$, $g_{9/2}$, $g_{7/2}$ and $d_{5/2}$ for proton and $h_{11/2}$, $g_{7/2}$, $d_{5/2}$, $d_{3/2}$ for neutron, among which the $h_{11/2}$ orbitals originate from the negative-parity subshell, while all the other orbitals originate from positive-parity subshells for both proton and neutron. In the other odd-odd Cs nuclei (*e.g.*, ^{122,124,128,130}Cs [7–10]) surrounding ^{126}Cs, while the two-quasiparticle yrast bands are commonly built on the positive-parity $\pi h_{11/2} \otimes \nu h_{11/2}$ configuration, the hitherto-known various two-quasiparticle yrare bands are mostly built on a negative-parity configuration which consists of either an $h_{11/2}$ proton coupled with a positive-parity neutron or an $h_{11/2}$ neutron coupled with a positive-parity proton. In contrast, those positive-parity bands built on the coupling between two valence quasiparticles both from the low-j positive-parity subshells have seldom been identified in the literature. This feature can be well understood through the striking difference in aligned angular momentum between the different single quasiparticles observed in odd-proton and -neutron nuclei of this region. In odd-proton nuclei of this region, *e.g.* in ^{127}Cs [11], the $h_{11/2}$ quasiproton is observed to carry a much larger aligned angular momentum than the other single quasiprotons available near the Fermi surface. The case is also true for the $h_{11/2}$ quasineutron (see, *e.g.*, ref. [12] for ^{127}Ba). Therefore, in an odd-odd nucleus of this region, bands having an $h_{11/2}$ quasiproton or $h_{11/2}$ quasineutron or both are expected to approach the yrast line more rapidly, thereby allowing such bands to be observed more easily in a heavy-ion–induced fusion-evaporation reaction. With this in mind, we have tentatively assigned negative parity to bands 3-6.

To further explore the possible configurations of bands 3-6, the alignment properties and energy staggering

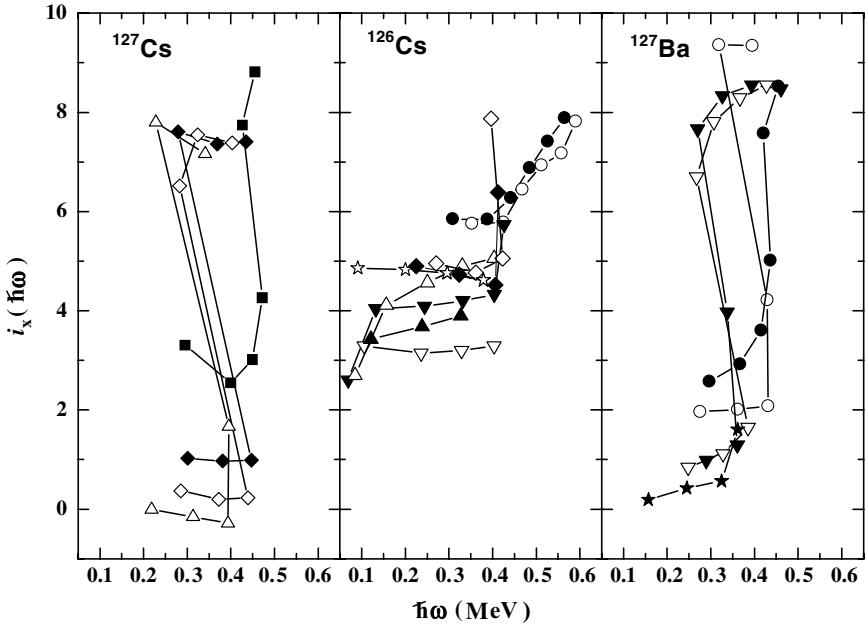

Fig. 2. Experimental alignments for the $h_{11/2}[550]1/2^-$ (■), $g_{7/2}[422]3/2^+$ (◇, ◆), and $d_{5/2}[420]1/2^+$ (△) bands in ^{127}Cs [11], the $h_{11/2}[523]7/2^-$ (○, ●), $d_{5/2}[402]5/2^+$ (▽, ▼) and $d_{3/2}[411]1/2^+$ (★) bands in ^{127}Ba [10], and bands 2 (○, ●), 3 (△, ▲), 4 (▽, ▼), 5 (◇, ◆), and 6 (☆) in ^{126}Cs. For ^{126}Cs (^{127}Cs and ^{127}Ba), open and closed symbols are used for $\alpha = 0$ and 1 ($\alpha = +1/2$ and $-1/2$), respectively. A common set of Harris parameters $J_0 = 17.0$ MeV$^{-1}\hbar^2$ and $J_1 = 25.8$ MeV$^{-3}\hbar^4$ is used for all bands above.

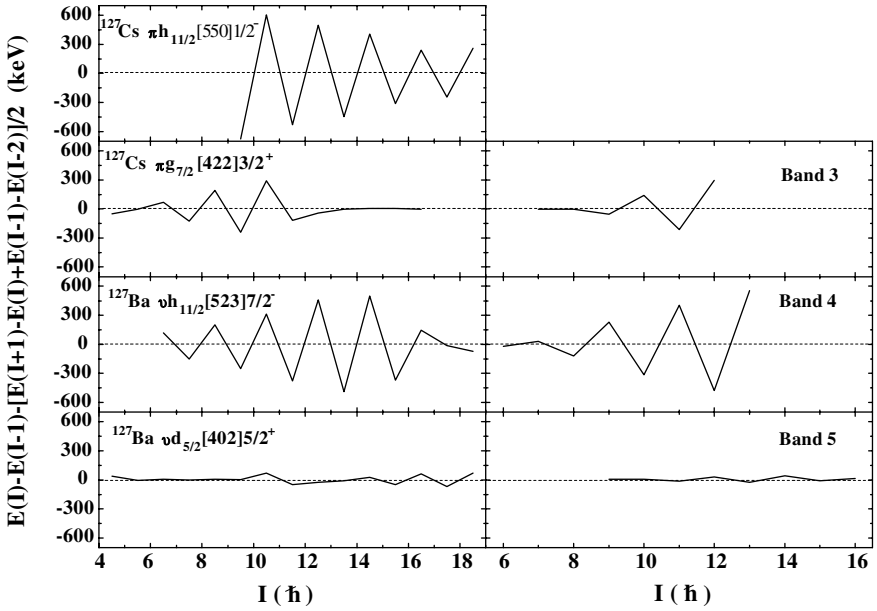

Fig. 3. $E(I) - E(I-1) - [E(I+1) - E(I) + E(I-1) - E(I-2)]/2$ *vs.* I plots for the near-yrast bands in ^{127}Ba [10], ^{127}Cs [11] and ^{126}Cs. Only bands where both signature partners are known have been selected.

properties of these bands have been studied and compared with those of the near-yrast bands observed in the odd-A neighbors ^{127}Cs [11] and ^{127}Ba [12]. The results are shown in figs. 2 and 3. Data of the near-yrast $\nu g_{7/2}[404]7/2^+$ band observed in another odd-A neighbor ^{125}Xe [13] is not included in figs. 2 and 3, but it can be stated that this band resembles the $\nu d_{5/2}[402]5/2^+$ band of ^{127}Ba in the presently interested properties. From figs. 2 and 3, it is seen that band 4 shows significant signature splitting in alignment and moderate energy staggering. A similar feature is seen also in the $h_{11/2}$ band of ^{127}Ba and the $g_{7/2}$ band of ^{127}Cs but not in the other bands of the odd-A neighbors (see figs. 2 and 3). This strongly suggests that the active participant (the quasiparticle that contributes to both of its two signatures) in the configuration of band 4 should be associated with either the $h_{11/2}$ neutron

Table 1. Energies, intensities, DCO ratios, and spin-parity assignments of the γ-transitions reported in fig. 1 for ^{126}Cs.

E_γ (keV) [a]	$I_\gamma^{(b)}$	DCO [c]	Assignment
Band 1			
362.0	7(1)	0.61(12)	$(12^+) \rightarrow (11^+)$
689.3	13(2)	0.97(14)	$(13^+) \rightarrow (11^+)$
327.2	6(2)	0.72(11)	$(13^+) \rightarrow (12^+)$
672.0	6(2)	1.10(24)	$(14^+) \rightarrow (12^+)$
771.2	8(1)	0.98(16)	$(15^+) \rightarrow (13^+)$
426.5	17(2)	0.58(10)	$(15^+) \rightarrow (14^+)$
901.6	< 2		$(16^+) \rightarrow (14^+)$
936.0	8(1)	0.97(17)	$(17^+) \rightarrow (15^+)$
461.0	< 2		$(17^+) \rightarrow (16^+)$
1007.8	6(1)		$(19^+) \rightarrow (17^+)$
1066.7	< 3		$(21^+) \rightarrow (19^+)$
Band 2			
140.8	88(5)	0.67(7)	$(10^+) \rightarrow (9^+)$
478.3	< 2		$(11^+) \rightarrow (9^+)$
337.5	51(4)	0.56(7)	$(11^+) \rightarrow (10^+)$
592.5	43(4)	1.00(9)	$(12^+) \rightarrow (10^+)$
254.5	36(3)	0.65(9)	$(12^+) \rightarrow (11^+)$
650.6	6(1)	1.04(16)	$(13^+) \rightarrow (11^+)$
395.7	38(3)	0.60(9)	$(13^+) \rightarrow (12^+)$
739.2	35(3)	1.01(10)	$(14^+) \rightarrow (12^+)$
343.2	8(1)	0.61(10)	$(14^+) \rightarrow (13^+)$
807.0	9(2)	0.95(13)	$(15^+) \rightarrow (13^+)$
463.5	18(2)	0.63(11)	$(15^+) \rightarrow (14^+)$
879. 0	22(2)	1.06(11)	$(16^+) \rightarrow (15^+)$
910.7	7(1)	0.99(18)	$(17^+) \rightarrow (15^+)$
495.6	8(1)	0.52(10)	$(17^+) \rightarrow (16^+)$
960.7	14(2)	0.99(14)	$(18^+) \rightarrow (16^+)$
993.3	5(1)	0.94(21)	$(19^+) \rightarrow (17^+)$
527.8	5(1)	0.68(18)	$(19^+) \rightarrow (18^+)$
1045.5	7(2)		$(20^+) \rightarrow (18^+)$
1072.3	4(2)		$(21^+) \rightarrow (19^+)$
554.5	< 3		$(21^+) \rightarrow (20^+)$
1135.1	4(2)		$(22^+) \rightarrow (20^+)$
1148.2	< 3		$(23^+) \rightarrow (21^+)$
1198.0	< 3		$(24^+) \rightarrow (22^+)$
Transitions between band 1 and 2			
637.8	7(1)	1.05(22)	$(11^+) \rightarrow (9^+)$
496.6	17(2)	0.57(9)	$(11^+) \rightarrow (10^+)$
95.6	4(1)		$(12^+) \rightarrow (11^+)$
520.8	19(2)	0.62(13)	$(12^+) \rightarrow (11^+)$
593.3	6(2)		$(13^+) \rightarrow (12^+)$
145.5	< 3		$(14^+) \rightarrow (13^+)$
542.3	18(2)	0.56(9)	$(14^+) \rightarrow (13^+)$
969.1	3(1)		$(15^+) \rightarrow (13^+)$
680.1	< 2		$(16^+) \rightarrow (14^+)$
637.1	6(1)		$(16^+) \rightarrow (15^+)$
277.8	< 3		$(18^+) \rightarrow (17^+)$

Table 1. Continued.

E_γ (keV) [a]	$I_\gamma^{(b)}$	DCO [c]	Assignment
Band 3			
128.6	8(1)	0.70(10)	$(6^-) \rightarrow (5^-)$
280.9	5(1)	0.95(19)	$(7^-) \rightarrow (5^-)$
152.4	16(3)	0.63(15)	$(7^-) \rightarrow (6^-)$
330.8	8(2)	0.92(24)	$(8^-) \rightarrow (6^-)$
178.3	16(2)	0.68(12)	$(8^-) \rightarrow (7^-)$
389.9	5(2)		$(9^-) \rightarrow (7^-)$
211.7	12(3)	0.53(11)	$(9^-) \rightarrow (8^-)$
562.3	4(1)		$(10^-) \rightarrow (8^-)$
350.8	4(1)		$(10^-) \rightarrow (9^-)$
570.4	11(2)	0.94(16)	$(11^-) \rightarrow (9^-)$
219.4	3(1)		$(11^-) \rightarrow (10^-)$
728.0	3(1)		$(12^-) \rightarrow (10^-)$
722.5	8(1)		$(13^-) \rightarrow (11^-)$
860.8	4(1)		$(15^-) \rightarrow (13^-)$
Band 4			
99.0	37(3)	0.60(8)	$(5^-) \rightarrow (4^-)$
210.6	< 2		$(6^-) \rightarrow (4^-)$
110.2	21(3)	0.57(9)	$(6^-) \rightarrow (5^-)$
272.7	3(1)		$(7^-) \rightarrow (5^-)$
161.4	21(3)	0.67(10)	$(7^-) \rightarrow (6^-)$
314.8	9(1)	1.00(15)	$(8^-) \rightarrow (6^-)$
153.4	19(3)	0.57(11)	$(8^-) \rightarrow (7^-)$
537.6	3(1)		$(9^-) \rightarrow (7^-)$
384.4	8(1)	0.67(16)	$(9^-) \rightarrow (8^-)$
539.7	17(2)	0.96(10)	$(10^-) \rightarrow (8^-)$
155.2	4(1)		$(10^-) \rightarrow (9^-)$
712.6	< 3		$(11^-) \rightarrow (9^-)$
557.4	5(1)		$(11^-) \rightarrow (10^-)$
708.8	11(1)	1.03(18)	$(12^-) \rightarrow (10^-)$
852.3	< 2		$(13^-) \rightarrow (11^-)$
846.4	7(2)		$(14^-) \rightarrow (12^-)$
882.1	3(1)		$(16^-) \rightarrow (14^-)$
Band 5			
87.7	9(2)	0.64(21)	$(7^-) \rightarrow (6^-)$
142.9	16(2)	0.64(14)	$(8^-) \rightarrow (7^-)$
353.7	5(1)		$(9^-) \rightarrow (7^-)$
210.8	14(2)	0.66(22)	$(9^-) \rightarrow (8^-)$
473.6	8(1)	0.96(12)	$(10^-) \rightarrow (8^-)$
262.8	10(1)	0.57(14)	$(10^-) \rightarrow (9^-)$
564.6	16(2)	1.12(17)	$(11^-) \rightarrow (9^-)$
301.7	10(1)	0.64(10)	$(11^-) \rightarrow (10^-)$
669.3	8(1)	0.90(13)	$(12^-) \rightarrow (10^-)$
367.7	7(2)	0.72(18)	$(12^-) \rightarrow (11^-)$
745.1	14(2)	1.07(14)	$(13^-) \rightarrow (11^-)$
834.2	6(1)		$(14^-) \rightarrow (12^-)$
442.0	< 2		$(14^-) \rightarrow (13^-)$
863.9	9(1)	1.11(24)	$(15^-) \rightarrow (13^-)$
807.3	4(1)		$(17^-) \rightarrow (15^-)$
Band 6			
185.6	5(1)	0.94(23)	$(7^-) \rightarrow (5^-)$
403.7	7(1)	0.97(12)	$(9^-) \rightarrow (7^-)$
594.5	8(1)	1.01(15)	$(11^-) \rightarrow (9^-)$
760.3	5(1)	0.96(28)	$(13^-) \rightarrow (11^-)$

Table 1. Continued.

E_γ (keV) [a]	$I_\gamma^{(b)}$	DCO [c]	Assignment
Transitions linking band 3 to band 4			
184.5	9(2)	0.55(15)	$(5^-) \rightarrow (4^-)$
85.5	< 3		$(5^-) \rightarrow (5^-)$
214.0	11(2)	0.48(11)	$(6^-) \rightarrow (5^-)$
256.1	4(1)	0.51(13)	$(7^-) \rightarrow (6^-)$
Transitions linking bands 5 and 6 to band 4			
262.7	5(1)	0.59(14)	$(5^-) \rightarrow (5^-)$
152.5	< 2		$(5^-) \rightarrow (6^-)$
353.1	7(1)	0.55(14)	$(6^-) \rightarrow (5^-)$
242.8	< 2		$(6^-) \rightarrow (6^-)$
Transitions between band 5 and 6			
90.4	< 3		$(6^-) \rightarrow (5^-)$
94.9	3(1)		$(7^-) \rightarrow (6^-)$
135.3	3(1)		$(8^-) \rightarrow (7^-)$
265.4	5(1)	0.58(12)	$(9^-) \rightarrow (8^-)$
208.2	3(1)		$(10^-) \rightarrow (9^-)$

[a] Accurate to 0.5 keV for most transitions and increases up to 1 keV for transitions with $I_\gamma < 5$.
[b] Obtained from a combination of singles and coincidence data, and normalized to the 218 keV transition ($I_\gamma = 100$) feeding the ground state (cf. ref. [1]).
[c] Deduced by gating on a $\Delta I = 2$ transition.

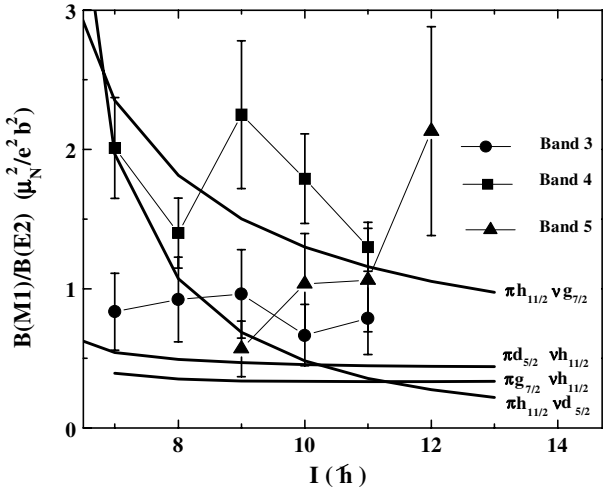

Fig. 4. Comparison of $B(M1)/B(E2)$ values measured for bands 3, 4 and 5 (symbols connected with thin solid lines) with those predicted for the configurations shown at the right-bottom corner (thick solid lines). Parameters used in the calculations of the predicted $B(M1)/B(E2)$ values: $Q_0 = 3.5$ eb, $g_R = 0.31$, $g_p(d_{5/2}) = 1.35$, $g_p(g_{7/2}) = 0.72$, $g_p(h_{11/2}) = 1.20$, $g_n(d_{5/2}) = -0.33$, $g_n(g_{7/2}) = 0.21$, $g_n(h_{11/2}) = -0.21$, $i_p(d_{5/2}) = 0.5$, $i_p(g_{7/2}) = 1.0$, $i_p(h_{11/2}) = 3.20$, $i_n(d_{5/2}) = 0.50$, $i_n(g_{7/2}) = 0.5$, $i_n(h_{11/2}) = 1.90$.

or the $g_{7/2}$ proton, and the inactive participant (the quasiparticle that contributes to only one of its two signatures) should be associated with a non-identical quasiparticle having opposite parity (to ensure that band 4 has negative parity) and larger signature splitting in energy (to ensure that this quasiparticle contributes only to its favored signature in the configuration of band 4). Hence, band 4 can be assigned to either the $\pi d_{5/2}(\alpha = +1/2)[420]1/2^+ \otimes \nu h_{11/2}(\alpha = \pm 1/2)[523]7/2^-$ or the $\pi g_{7/2}(\alpha = \pm 1/2)[422]3/2^+ \otimes \nu h_{11/2}(\alpha = -1/2)[523]7/2^-$ configuration. Likewise, candidates for configurations of bands 3, 5 and 6 can be deduced as follows: $\pi g_{7/2}(\alpha = \pm 1/2)[422]3/2^+ \otimes \nu h_{11/2}(\alpha = -1/2)[523]7/2^-$ or $\pi d_{5/2}(\alpha = +1/2)[420]1/2^+ \otimes \nu h_{11/2}(\alpha = \pm 1/2)[523]7/2^-$ for band 3, $\pi h_{11/2}(\alpha = -1/2)[550]1/2^- \otimes \nu g_{7/2}(\alpha = \pm 1/2)$ $[404]7/2^+$ or $\pi h_{11/2}(\alpha = -1/2)[550]1/2^- \otimes \nu d_{5/2}(\alpha = \pm 1/2)$ $[402]5/2^+$ for band 5 and $\pi h_{11/2}(\alpha = -1/2)[550]1/2^- \otimes \nu d_{3/2}(\alpha = -1/2)[411]1/2^+$ for band 6. The assignments for the coupled bands have also been checked through a comparison of their experimental in-band $B(M1; I \rightarrow I-1)/B(E2; I \rightarrow I-2)$ ratios with those predicted from the geometrical model [14] for various possible configurations. This comparison is shown in fig. 4. It is seen that the experimental $B(M1)/B(E2)$ ratios of band 3 are observed to be overall smaller than those of band 4, and correspondingly, the calculated $B(M1)/B(E2)$ ratios are overall smaller for the $\pi g_{7/2} \otimes \nu h_{11/2}$ configuration than for the $\pi d_{5/2} \otimes \nu h_{11/2}$ configuration. In view of this similarity, we suggest that bands 3 and 4 are built predominantly on the $\pi g_{7/2} \otimes \nu h_{11/2}$ and $\pi d_{5/2} \otimes \nu h_{11/2}$ configurations, respectively.

As band 4 is thought to be built on the $\pi d_{5/2} \otimes \nu h_{11/2}$ configuration, it can be expected from the additivity law of the cranked shell model (CSM) [15] that the favored signature of this band is $\alpha_f = 1/2 \times (-1)^{5/2\text{-}1/2} + 1/2 \times (-1)^{11/2\text{-}1/2} = 0$. In other words, the even-spin sequence is expected to lie lower in energy than the odd-spin sequence at higher spins. Experimentally, the sequence connected by the 210, 314, 540, 708 and 846 keV $E2$ transitions in band 4 is observed to lie pronouncedly lower in energy than the another sequence, as can be inferred from figs. 1 and 3; therefore, the bandhead of band 4 is considered to have an even-spin value. According to the Gallagher-Moszkowski coupling rule [16] for odd-odd nucleus, $K = 3$ or 4 is expected for the $\pi d_{5/2}[420]1/2^+ \otimes \nu h_{11/2}[523]7/2^-$ configuration, yielding a lower limit of 3 for the bandhead spin value of band 4. On the other hand, there are some clear indications that the bandhead spin value should be no more than 5. In the used reaction, band 2 was observed to be the most strongly populated band in ^{126}Cs, and bands 3-6 were populated with similar intensities (cf. table 1). This indicates that, just like in the surrounding odd-odd Cs isotopes [7–10], the $\pi h_{11/2} \otimes \nu h_{11/2}$ band is the yrast band in ^{126}Cs. If the bandhead spin value of band 2 is 9 or lower as proposed in refs. [1,2], a spin assignment larger than 5 $\hbar$ for the bandhead of band 4 would result in a situation that band 2 is no longer the yrast band in ^{126}Cs inconsistent with the observation. Taking the above considerations into account, we have tentatively assigned

the bandhead spin of band 4 as 4 $\hbar$. On this basis, the spins of the other states in bands 3-6 have been deduced from the measured DCO data, as shown in fig. 1.

With the assigned spins for band 5, the odd-spin sequence ($\alpha = 1$) of this band is found to lie lower in energy than the even-spin sequence partner ($\alpha = 0$) at higher spins. This feature tallies with the expectation from the additivity law of CSM [15] for the $\pi h_{11/2} \otimes \nu g_{7/2}$ configuration but not for another candidate configuration, *i.e.* the $\pi h_{11/2} \otimes \nu d_{5/2}$ configuration, thus favoring the $\pi h_{11/2} \otimes \nu g_{7/2}$ configuration assignment for band 5. With the present spin assignments for bands 3-6, no signature inversion is observed in these negative-parity bands, unlike in the $\pi h_{11/2} \otimes \nu h_{11/2}$ band, which shows low-spin signature inversion as discussed in ref. [2].

This work is supported by the Major State Basic Research Development Programme of China (Contract. No. G2000077400) and the National Natural Science Foundation of China under grant Nos. 19775019, 19975022 and 10205006.

References

1. T. Komatsubara *et al.*, Nucl. Phys. A **557**, 419c (1993).
2. Y.-Z. Liu *et al.*, Phys. Rev. C **58**, 1849 (1996).
3. T. Koike *et al.*, Phys. Rev. C **64**, 061304(R) (2001).
4. K. Starosta *et al.*, Phys. Rev. Lett. **86**, 971 (2001).
5. X.-F. Li *et al.*, Chin. Phys. Lett. **19**, 1779 (2002).
6. T. Komatsubara *et al.*, University of Tsukuba Tandem Accelerator Center Annual Report (1991) p. 25
7. C.-B. Moon, T. Komatsubara, K. Furuno, Nucl. Phys. A **674**, 343 (2000).
8. A. Gizon *et al.*, Nucl. Phys. A **694**, 63 (2001).
9. E.S. Paul *et al.*, Phys. Rev. C **40**, 619 (1989).
10. Y.-J. Ma *et al.*, University of Tsukuba Tandem Accelerator Center Annual Report (2001) p. 30
11. D. Ward *et al.*, Nucl. Phys. A **539**, 547 (1992).
12. Y. Liang *et al.*, Phys. Rev. C **42**, 890 (1990).
13. A. Granderath *et al.*, Nucl. Phys. A **524**, 153 (1991).
14. F. Dönau, Nucl. Phys. A **471**, 469 (1987).
15. R. Bengtsson, S. Frauendorf, Nucl. Phys. A **329**, 139 (1979).
16. C.J. Gallagher, S.A. Moszkowski, Phys. Rev. **111**, 1282 (1958).